ELECTRONIC STRUCTURE AND THE STABILITY OF METAL ALLOYS: CRYSTALS, IONIC/METALLIC GLASSES and QUASICRYSTALS

Ion C. Baianu

FSHN & NPRE Departments, UIUC

***Illinois Geometry Laboratory*: A Quasicrystal Stability Group presentation**

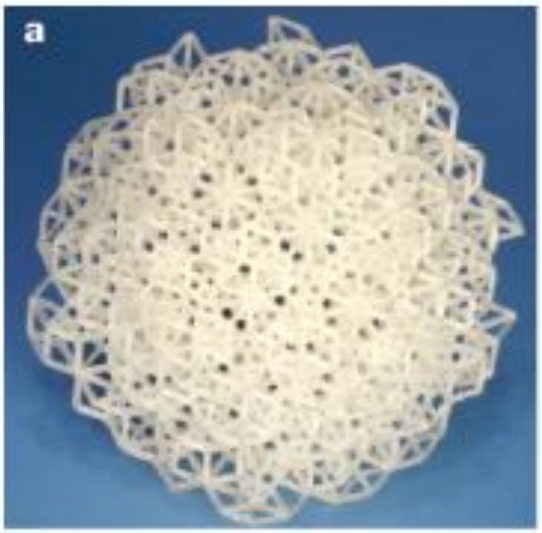

A 3D-Printed Model of a 694-cell Photonic Icosahedral Quasicrystal

[High-res. Stereolitographic (SLA-250) model in plastic of an icosahedral quasicrystal, Source: W. Man et al., *Nature*, 2005:1 doi:10.1038/nature03977].

- **The first reported quasicrystalline structure was that of a metal alloy $Al_{0.14}Mn_{0.86}$ with icosahedral point symmetry** (Schechtman, D. et al. 1984**.** "Metallic Phase with Long-Range Orientational Order and No Translational Symmetry"**,** ***Phys.Rev. Lett.*****, 53:** 1951-1953**.**
  Comment: Paul J. Steinhardt, 1986. *Distinguishing a* **Quasicrystal** *from an* **Icosahedral Glass** Via *Lattice Imaging*, ***Phys. Rev. Lett***. **57**: 2769)**.**
  - **This is where the quasicrystal story began, … or has it ?!**

1. CRYSTALS and LATTICES

A *crystal* is a regular structure with long-range order and a single periodic unit (cell) that by exact repetition forms a lattice **with both rotational and translational symmetry.**

- **The *lattice* is a mathematical concept.**
  - **In Geometry and Abstract Algebra--Group Theory a *lattice* in $\mathbb{R}^n$ is a discrete subgroup of $\mathbb{R}^n$ which spans the real vector space $\mathbb{R}^n$**
  - $$\Lambda = \left\{ \sum_{i=1}^{n} a_i v_i \;\middle|\; a_i \in \mathbb{Z} \right\}$$
    where $\{v_1, \ldots, v_n\}$ is a basis for $\mathbb{R}^n$.

- In the context of Crystallography**,** Material Science and Solid-state physics, a **lattice** is a synonym for the "frame work" of a crystalline structure, a 3-dimensional array of regularly spaced points coinciding with the atom or molecule positions in a crystal.
  - Thus, a crystal *lattice* is a discrete, periodic arrangement of points in *n* dimensions larger than (or equal to) 1 and less than or equal to 3; its points are the atoms (or ions) that make up the crystal.

1a. An Example

A Face Centered Cubic (fcc) Crystalline Cluster and Lattice

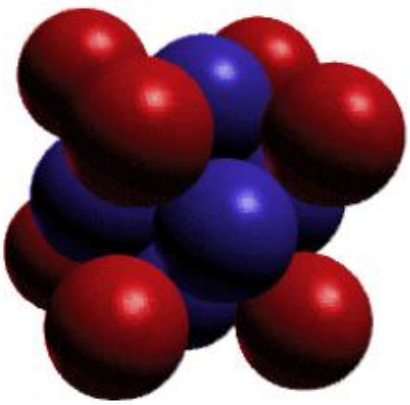

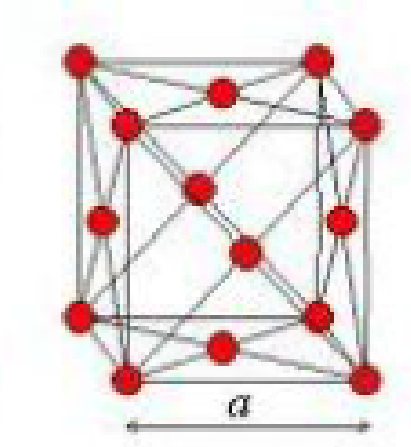

----➔

Idealized, Discrete Geometry

Regular OCTAHEDRON

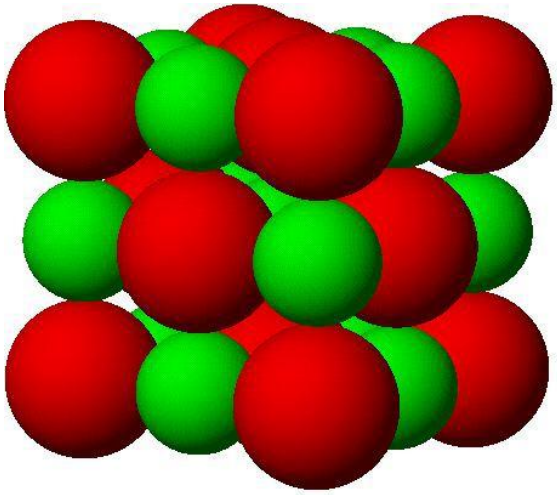

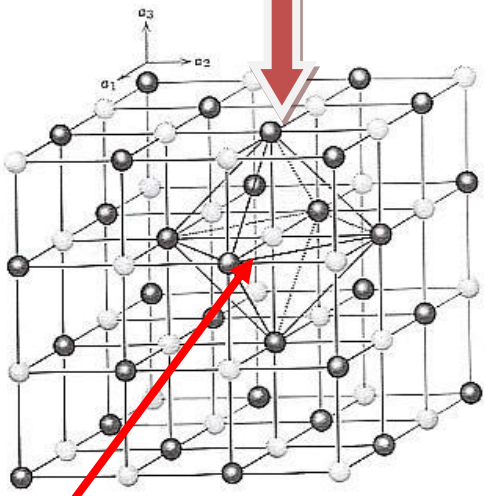

X-ray Diffraction (FT, or FFT)

1a. A truncated Octahedron (in *reciprocal* (FT) space)

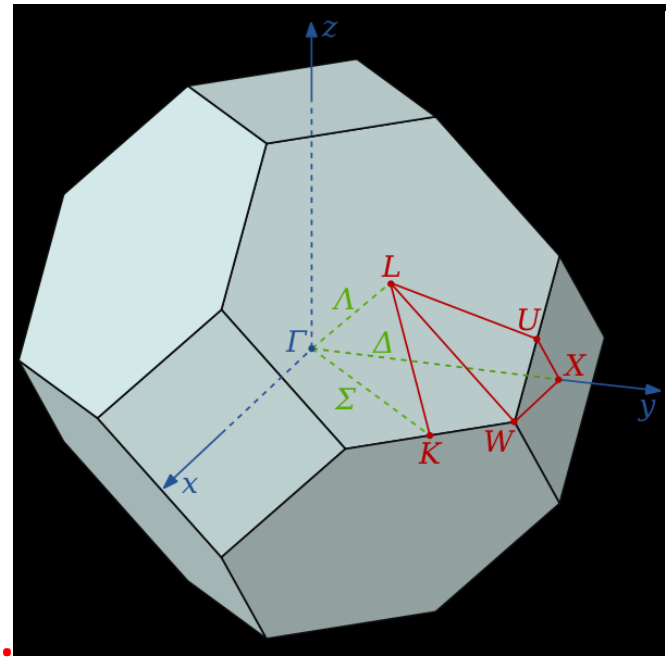

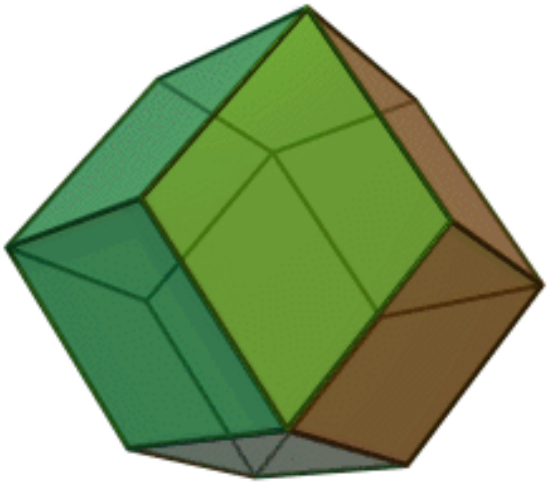

1a. **1b.**

1a. **The first Brillouin zone of a face-centred cubic (FCC) lattice, with its points of high symmetry marked; its symmetry group is O_h.**

1.b. **For the BCC lattice the first Brillouin zone is a rhombic dodecahedron.**

1c. The Brillouin Zones

FT or FFT

Crystal Lattice ---------→ **Reciprocal Lattice**

<---- FT^{-1}

A SIMPLIFIED, 2D- REPRESENTATION

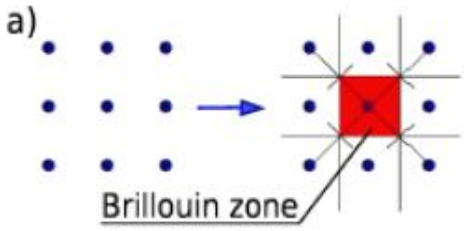

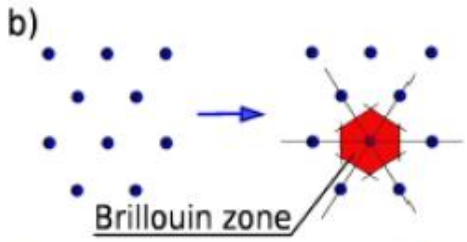

The reciprocal lattices (dots) and corresponding first Brillouin zones of (a) square lattice and (b) hexagonal lattice.

- **Mathematically,** *the Brillouin zone* is the **Voronoi cell** around the origin of the reciprocal lattice.
- **Physically,** ***the Brillouin zone*** *turns out to be very important for understanding the electronic structure of crystals*. It is defined by the set of points in *reciprocal* **(**or **k-)** space that are closest to the origin of **k**-space without crossing any Bragg planes.

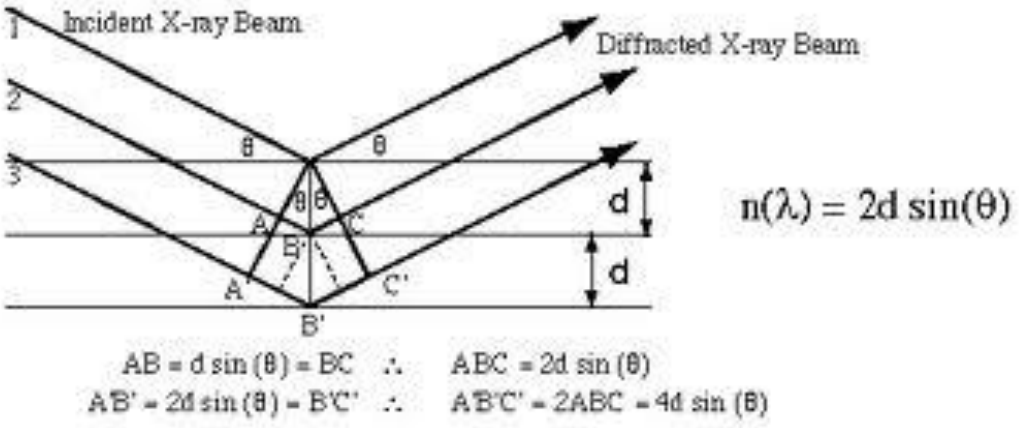

Cubic lattice system CUB(1),FCC(1), BCC(1)

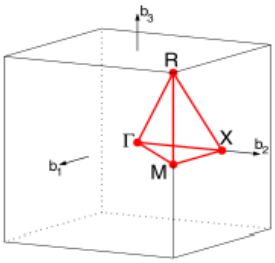

CUB path: Γ-X-M-Γ-R-X|M-R

[Setyawan & Curtarolo, DOI: 10.1016/j.commatsci.2010.05.010]

Simple Cubic Lattice (CUB) BZ.

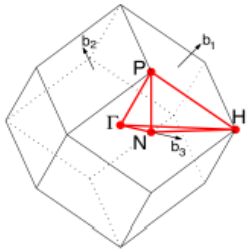

BCC path: Γ-H-N-Γ-P-H|P-N

[Setyawan & Curtarolo, DOI: 10.1016/j.commatsci.2010.05.010]

Body Centered Cubic Lattice (BCC) BZ.

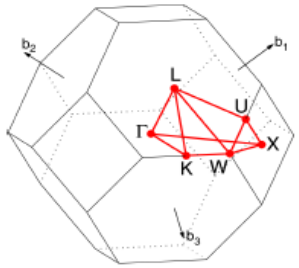

FCC path: Γ-X-W-K-Γ-L-U-W-L-K|U-X

[Setyawan & Curtarolo, DOI: 10.1016/j.commatsci.2010.05.010]

Face Centered Cubic Lattice (FCC) BZ.

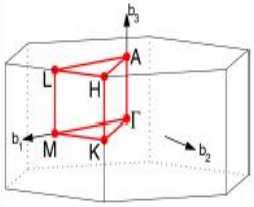

HEX path: Γ-M-K-Γ-A-L-H-A|L-M|K-H

[Setyawan & Curtarolo, DOI: 10.1016/j.commatsci.2010.05.010]

Hexagonal Lattice (HEX) BZ.

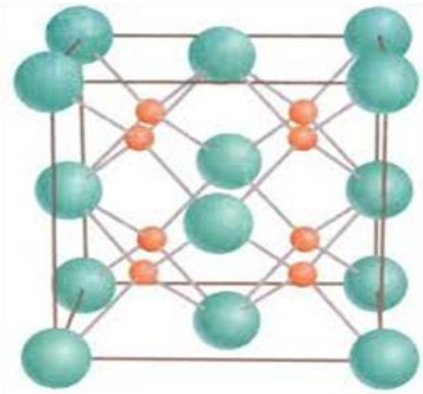

Face-centered-cubic (fcc) crystal structure of PuO_2 (Pu atoms in green, O atoms in red).

HCP

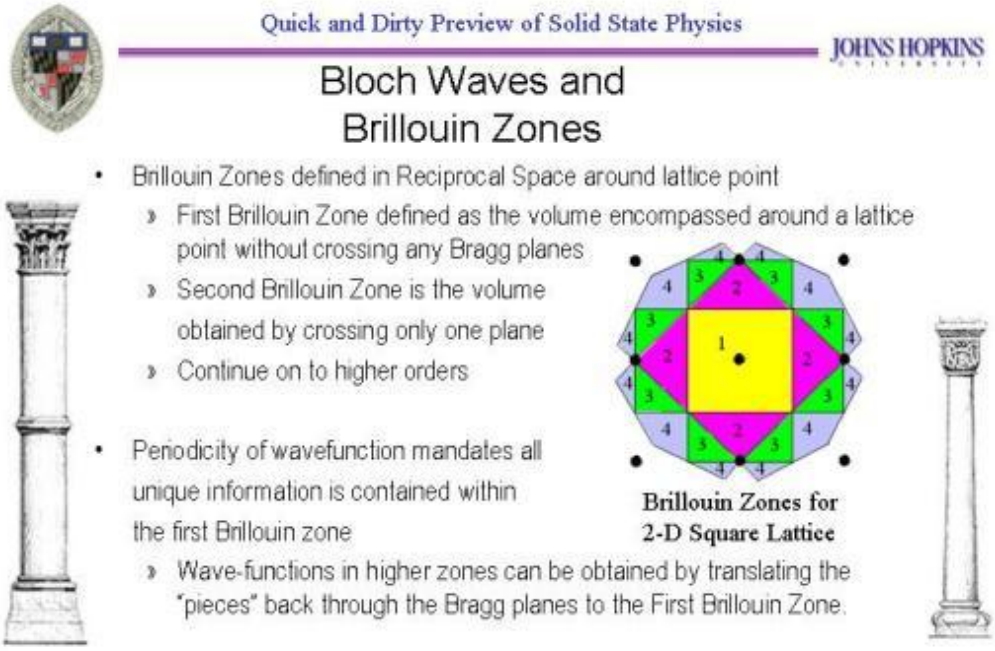

2. STABILITY and Electron Distributions for METAL ALLOYS

2.a. The concept of a Cohesive Energy in a solid

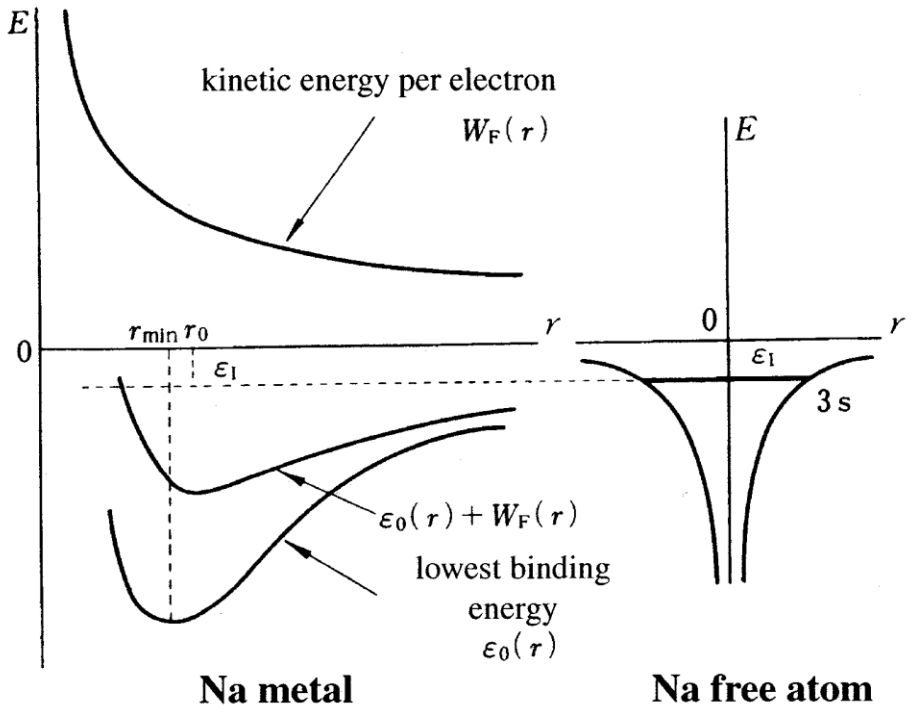

The curve $\mathcal{E}_0(\mathbf{r})$ represents the lowest energy of electrons with the wave vector **k**=0 while the curve $\boldsymbol{\varepsilon}_{kinetic}$ represents an average kinetic energy per electron. $\boldsymbol{\varepsilon}_{ioniz}$ represents *the ionization energy* needed to remove the outer *3s* electron in a *free Na* metal to infinity and $\boldsymbol{\varepsilon}_c$ is **the cohesive energy**. (*THE BOSS*!)

The position of the minimum in the cohesive energy gives *an equilibrium interatomic distance* r_0. Gaps, or voids, between atoms would increase this distance and decrease the system's stability.

⇩

2.b. *How are electrons distributed in Metals and Metal Alloys ?*

How inter-metallic bonds or valence electrons *contribute to the metal alloy stability ?*

(Assuming, of course, that all atoms are as *closely packed* as physically possible!)

First, we choose a suitable coordinate, or 3D reference frame for the electrons, which is usually selected in the *k-space*, or the space of the wave vectors of the electron wave functions in a crystal and thermal vibrations of a lattice.

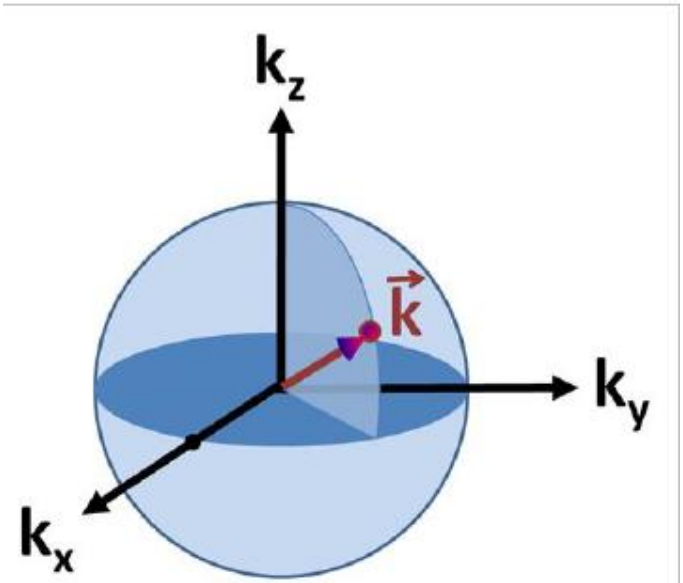

Figure 1: Spherical surface in *k*-space for electrons in three dimensions.

- In metallic and inter-metallic materials (*alloys*, for example) the metal ions are thought to be located at the crystal lattice points and to share a large number of energetic electrons that behave like a *nearly* **`free-gas'** of Fermions with a ***density of states*** **(DOS)** which is continuous throughout the crystal. For a free electron gas this is a *parabola* **up to the Fermi level (or gap), E_F!**

DOS := *NUMBER OF ELECTRONIC STATES per ENERGY INTERVALS* that are available to the electrons:

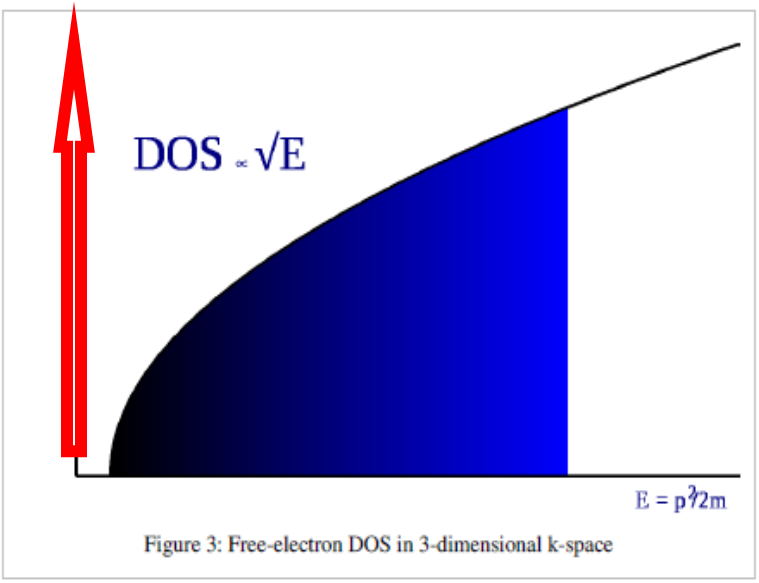

Figure 3: Free-electron DOS in 3-dimensional k-space

$E=p^2/2m$ →

Because of the periodicity of the crystal lattice there are ***Bloch waves*** of the electrons in the crystalline metals whose behavior can be completely characterized by considering *only* the first Brillouin zone. Therefore, the stability of the metal might be related to the intersection of the DOS at the Fermi level with the face of the Brillouin zone (Jones, 1936; Mott and Jones, 1937), i.e., as long as the DOS is *within*, (or at) the Brillouin zone the metallic crystal is stable. Hume-Rothery was very happy with this explanation until Brian Pippard showed that the DOS in $\mathbf{Cu_5Sn_8}$ alloys extended well beyond the first Brillouin zone [110] face **!**

At the Fermi level there opens a Fermi (or Jones) gap in the DOS -- **the DOS has a minimum at the Fermi energy –so called *"pseudogap"*-- in most metal alloys.**

[**Remark**: In graphite layers and MOSFET type devices there is a *2D- free electron gas* (**2DEG**)!]

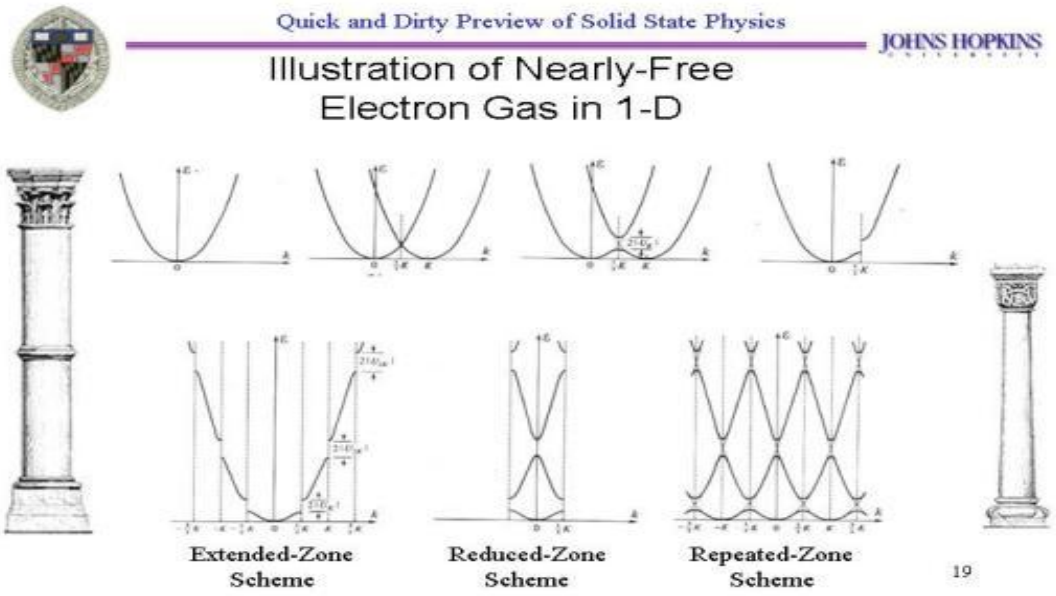

A little basic, 101 Chemistry:

- The arrangement of electrons in the (electron) orbitals of an atom is called the **atom's electron configuration**.
- One uses the **Pauli exclusion principle (**"An orbital can hold at most ONLY 2 electrons" ↓↑ = **up-down** spin pair **-> total spin is zero**) **and the Aufbau 'principle' or rules** to arrange the electrons in stable electron orbitals of an atom:
  - **Electrons are placed in the lowest energetically available subshell**
  - If two or more energetically equivalent orbitals are available (e.g., **p**, **d**, **f** etc.) then electrons should be **spread out between subshells** before their spins are paired up (**Hund's rule**)

Summary: When filled, the # of electrons in orbitals is: s 2 | p 6 | d 10 | f 14 …

The lowest energy levels are the most stable and are therefore filled up first !

2.c. The Possible Connection with the Hume-Rothery Rule for the Average # of Valence Electrons/atom (e/a) in metal alloys

(Jones, 1936; Mott and Jones, 1937; Evans, et al. 1979; Mizutani, U., 2008, 2010)

"The discovery of quasicrystal phases and (their) approximants in the **Al(rich)-Mn** system has revived the interest for complex aluminides containing transition-metal atoms.

- On the one hand, it is now accepted that **the Hume-Rothery stabilization plays a crucial role**.
- On the other hand, **transition-metal atoms have also a very important effect on their stability and their physical properties**. [Guy Trambly De Laissardière (LPTM, **CNRS**), Duc Nguyen-Manh, Didier Mayou (LEPES, **UKAEA**; *Submitted on 20 **Oct 2004** (v1), last revised 3 May 2005 (this version, v2)):* http://arxiv.org/abs/cond-mat/0410513].

2.d. Hume-Rothery Rule No. 2 (cca. 1926) :

***Metal alloys are* stable *for certain precise values of the* average (total) number of valence electrons per atom := e/a.**

Example : $Cu_5 Sn_8$ has a *stable bcc* structure for a value of e/a= 1.615... = (5x1 + 8x2)/(5+8) = 21/13 ! (The *Cu* atoms valence is taken to be 1 !)

Cu_xAl_{1-x} → e/a =7/5 =1.40 => *f.c.c* ; e/a =21/13/=1.62 => *b.c.c* ; e/a= 9/5= 1.80 =>*h.c.p*.

Al(rich)–TM quasicrystals and related phases are now also considered as *Hume-Rothery alloys* !

[Transition-metal atoms (TM atoms) are: TM = **Ti, V, Cr, Mn, Fe, Co, and Ni**.]

- In the literature, there are lots of theoretical studies-- from first-principles (*ab initio*)— of the electronic structure of **Al(rich)–TM crystals** and **Al(rich)–TM crystalline approximants of quasicrystals**.
  - **At low energy, the total DOS is nearly-free electrons like**-- their states are mainly sp **states** of the **Al** atoms.
  - The *d*–states of TM (TM = Ti, V, Cr, Mn, Fe, Co, Ni) are observed in the middle of the *sp* band.
  - In phases containing ***Cu*** atoms, the *d* peak of ***Cu*** is **strong** and it is located at an energy lower than that of *d*–peak of TM.

Guy Trambly De Laissardière et al (2005): ***"Electronic structure of complex spd Hume-Rothery phases in transition-metal aluminides."*** **[** in **The Science of Complex Alloy Phases**, USA, (2005) p. 345-374]:

``*In this paper, we review studies that unify the* classical Hume-Rothery stabilization for ***sp*** *electron phases with the virtual bound state model for transition-metal atoms embedded in the aluminum matrix. These studies lead to a new theory for "**spd** electron phases". It is applied successfully to* ***Al(Si)--transition-metal alloys*** ***and it gives a coherent picture of their stability and other physical properties."***

- ``*These results are based on first-principles (**ab initio**) calculations of the electronic structure and simplified models, compared to experimental results."*

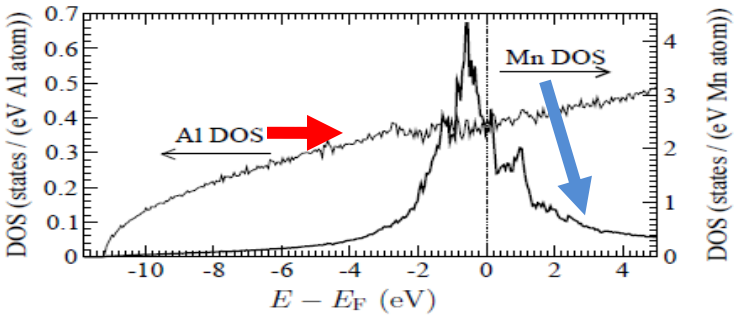

Figure 2: Non-magnetic DOS in a $Al_{107}Mn$ model. Mn atoms are in substitution to Al atoms in an Al f.c.c. Al(1) and Mn atoms are first-neighbors.

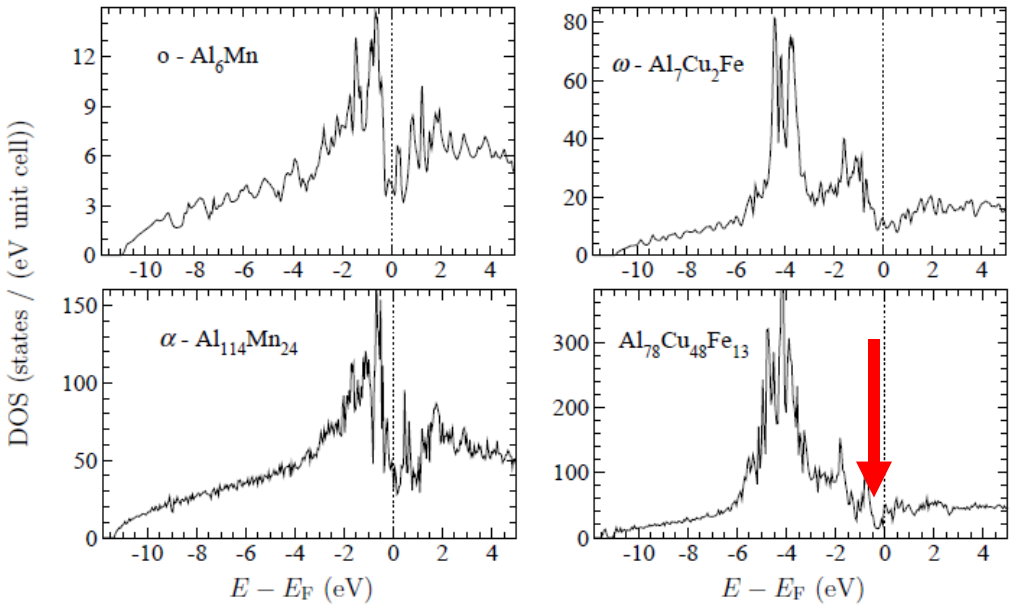

Figure 1: LMTO total DOS orthorhombic of o-Al_6Mn, tetragonal ω-Al_7Cu_2Fe, cubic α-Al–Mn and cubic α'-Al–Cu–Fe [13].

Ab initio Quantum Computations for ***spd*** Hume-Rothery Metal Alloys.

- **The red arrow points to the calculated Fermi pseudogap in the DOS !**

2.e. DOS of *spd* electron orbital Phases: *sp—d* hybridization

<< "

In many transition-metal aluminides, the Fermi level E_F is found near a large valley in the DOS that splits the band between bonding states and anti-bonding states (figure 1). This valley, called *"pseudogap"*, is generally attributed to a combined effect including the electron diffraction by the Bragg planes of a prominent Brillouin zone and a strong Al(*sp*)–**hybridization." >>**

Experimental Photo-emission Spectroscopy and specific heat measurements have confirmed the presence of a Fermi **pseudogap** in the DOS of many **Al–TM quasicrystals and their crystalline approximants**.

"The spd *aluminides are characterized by a* ***strong*** sp–d ***hybridization*** *between the* Al sp states and the TM d-orbitals. *Many experimental studies of photoemission spectra have shown this property (E. Belin-Ferr´e...) It is illustrated from the LMTO calculation through the comparison between the DOS's calculated with the sp–d hybridization ("exact" calculation) and the DOS' s calculated by setting to zero the matrix elements of the Hamiltonian that correspond to the* sp–d hybridization (calculation `*without sp–d hybridization*' [19]). *The width of the TM DOS is strongly reduced in the calculation without* sp–d hybridization *with respect to the exact calculation. Indeed the width of the TM DOS* (mainly d-state DOS) *is proportional to the square of the matrix element that couples the* d-states and the sp-states *in the (quantum) Hamiltonian*." [Guy Trambly De Laissardière (LPTM, **CNRS**) et al, 2005].

`*Negative valence*' of transition-metal atoms

In his original work on ***negative valence***, Raynor [1] assumed a transfer of electrons from the conduction band (sp band) to the d band in order to compensate the unpaired spins of the TM elements, and fill the d band. In this scheme the TM atoms remove electrons from the sp band and thus have a ***negative valence***.

``But a transfer of several electrons on one atom is unrealistic in metallic alloys since it corresponds to a **too large electrostatic energy for metallic alloys** [2].

The LMTO results allow to solve this paradox and to understand the **apparent negative valence of TM** in Al–TM compounds. Indeed, there is an increase of the sp DOS below E_F as compared to the free electron DOS due to the combined effect of sp–d hybridization and the diffraction of sp states by Bragg planes. In this scheme filling these additional sp states below E_F plays the same role as filling of the d band in Raynor's scheme. It results in an apparent negative valence of TM. Contrary to the d orbitals **these additional sp states are delocalized and do not lead to a strong electrostatic energy**. Yet one may expect that these additional sp states are linked to the TM atom and that they follow its displacement. This could explain the ***anomalous effective charge of TM elements as deduced from optical conductivity*** **[24]."**

Table 2: Negative valence of transition-metal elements in Al(rich) alloys: According to Raynor [1] and quantity $(-\Delta N_{sp})$ calculated from LMTO [14].

	Cr	Mn	Fe	Co	Ni
Raynor	−4.66	−3.66	−2.66	−1.66	−0.66
LMTO	−3.2 ($Al_{12}Cr$)	−2.7 ($Al_{12}Mn$) −2.0 (Al_6Mn)	−2.5 (Al_7Cu_2Fe)	−1.3 (Al_9Co_2) −0.9 (Al_5Co_2)	−1 (Al_3Ni)

2.f. Generalization of the Jones theory for the *spd* electron phases

"*Following a classical approximation* [5, 6] *for* Al(Si)-Mn alloys, *a simplified model is considered where* sp states are **nearly-free** and d states are **localized** on Mn sites i.
The* effective Hamiltonian *for the sp states is thus written as :

$$H_{eff(sp)} = \frac{\hbar^2 k^2}{2m} + V_{B,eff}$$

where $V_{B,eff}$ is *an effective Bragg potential* that takes into account the scattering of sp-states by the strong potential of **Mn** atoms. $V_{B,eff}$ depends thus on the positions r_i of Mn atoms.
By assuming that all Mn atoms are equivalent (and `avoid' each other !), one obtains:

$$V_{B,eff}(\mathbf{r}) = \sum_{\mathbf{K}} V_{B,eff}(\mathbf{K}) e^{i\mathbf{K}.\mathbf{r}}, \quad (10)$$

$$V_{B,eff}(\mathbf{K}) = V_B(\mathbf{K}) + \frac{|t_{\mathbf{K}}|^2}{E - E_d} \sum_i e^{-i\mathbf{K}.\mathbf{r}_i}, \quad (11)$$

where the vectors $\mathbf{K}$ belong to the reciprocal lattice, $t_{\mathbf{K}}$ is a average matrix element that couples sp states $\mathbf{k}$ and $\mathbf{k}-\mathbf{K}$ via the sp–d hybridization, and E_d is the energy of d states. The term $V_B(\mathbf{K})$ is a weak potential independent of the energy E. It corresponds to the Bragg potential for sp Hume-Rothery compounds.

The last term in equation (11), is due to the d-resonance of the wave function by the potential of Mn atoms. It is strong in an energy range $E_d - \Gamma \leq E \leq E_d + \Gamma$, where 2Γ is the width of the d DOS. This term is essential as it does represent the diffraction of the sp electrons by a network of d orbitals, i.e. the factor $\left(\sum_i e^{-i\mathbf{K}.\mathbf{r}_i}\right)$ corresponding to the structure factor of the TM atoms sub-lattice. As the d band of Mn is almost half filled, $E_F \simeq E_d$, this factor is important for energy close to E_F. Note that the Bragg planes associated with the second term of equation (11) correspond to Bragg planes determined by diffraction.

This qualitative analysis suggests that both sp–d hybridization and diffraction of sp states by the sub-lattice of Mn atoms are essential to understand the electronic structure of Al(Si)-Mn alloys. The strong effect of sp–d hybridization on the pseudogap is then understood in the framework of Hume-Rothery mechanism. "

2.g. Structural Stability of complex *spd* electron phases

``

Although there have been several first-principles calculations for different Al(rich)–TM compounds and related quasicrystalline phases, it is desirable to elucidate why the quasicrystalline phase is stable only by forming with TM of group VIIA (Mn, Re) and group VIIIA (Fe, Ru, Os, Co, Rh, Ir, Ni)? It is also essential to know whether these calculations confirm (or not) a Hume-Rothery mechanism for stabilizing spd compounds like that has been shown for simple sp compounds.

By using a Rigid Band Approximation within *local Density Functional theory*,
the effect of the average *number of (valence) electrons per atom,* e/a, on the relative stability has been studied [18].

This shows ("figure 7" of source) that transition-metal trialuminides go from the tetragonal **Al_3TM** structure to the monoclinic $Al_{13}TM_4$ structure as a function of the average electron number per atom ratio: **TETRAGONAL** (**1.5**) --→ **MONOCLINIC** (?)--→ Al_6Mn ***icosahedral*** quasicrystal (~**2.15**)

❖ The **Al_3TM type** structure is **more stable** for transition-metal trialuminides with **TM** at the beginning of the d series (Sc, Ti, V, Y, Zr, Nb, La, Hf, Ta),…. **e/a =? (3x3 - 3) / 4 = 1.50 ,** whereas

❖ the **$Al_{13}Fe_4$ type** structure is **more stable** for the transition-metal trialuminides with TM = Mn, Fe, Co, Ni Tc, Ru, Rh, Pd, Re, Os, Ir and Pt [18]. **e/a = ?...left as an exercise !**
Does the actual monoclinic structure agree with that expected for the *e/a* value of …?

❖ These theoretical predictions of the relative stability of the **transition-metal trialuminides** between the simple **tetragonal Al_3TM** structure and the more complex **monoclinic $Al_{13}TM_4$** structure, **agree with the Hume-Rothery condition for stabilization in terms of e/a**.

❖ For the Al_6Mn *icosahedral* quasicrystal, **e/a** is: (6x3 - 2)/7 = 16/7 = 2.286, or **2.0** if ***Val_Mn*** = - **4** !, whereas for other quasicrystals **e/a** = **1.75 ! [close to the $Al_{13}Fe_4$ value…?]**

❖ Concerning the DOS, it results that the consequences of the Hume-Rothery rules for the **transition-metal trialuminides** are the same as for the simpler sp electron compounds:

The most stable phases are those for which E_F is located in a *pseudogap* of the total DOS. "

E_F := Fermi level

ACKNOWLEDGMENTS:

Fruitful discussions and suggestions from Professor Florin Boca and Professor James F. Glazebrook of our Mathematics Department –as well as valuable references to articles pertinent to the theme of **aperiodic** systems—are hereby gratefully acknowledged.

Hamlet: ***"And therefore as a stranger give it welcome.***
There are more things in heaven and earth, Horatio*, than are dreamt of in your philosophy."*

Further Reading: The solid-state `pin-ball machine'

European Network of Excellence

European School in Materials Science

The Hume-Rothery rules for Structurally Complex Alloy Phases

Uichiro Mizutani

Toyota Physical & Chemical Research Institute, Japan

The 3rd Euroschool 2008, Ljubljana, Slovenia
Complex Metallic Alloys: Surfaces and Coatings
May 29, 2008

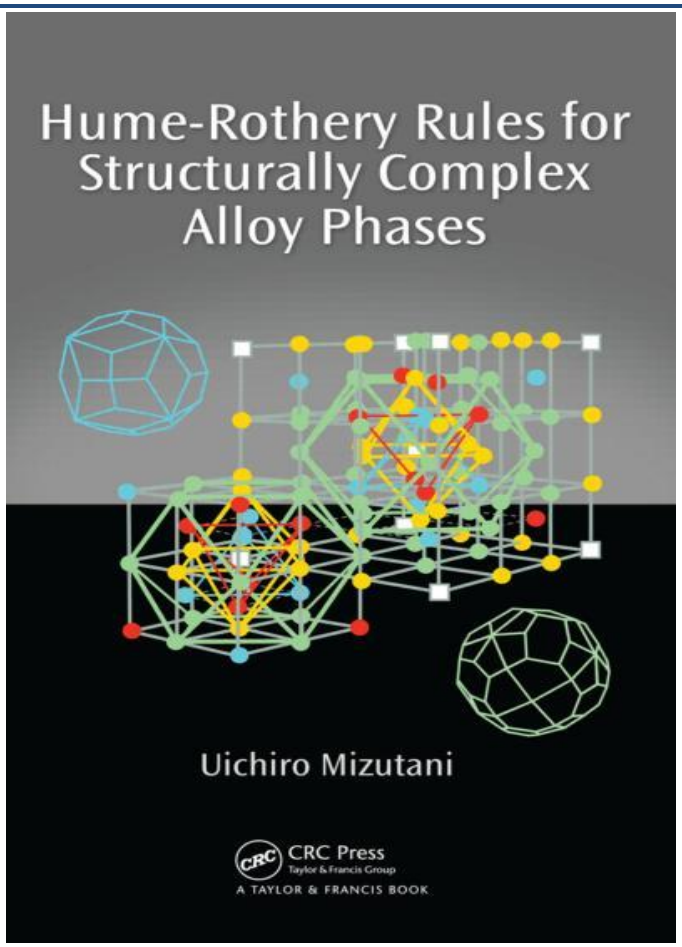

3. QUASICRYSTALS

3.1. AlNiCo Quasicrystals

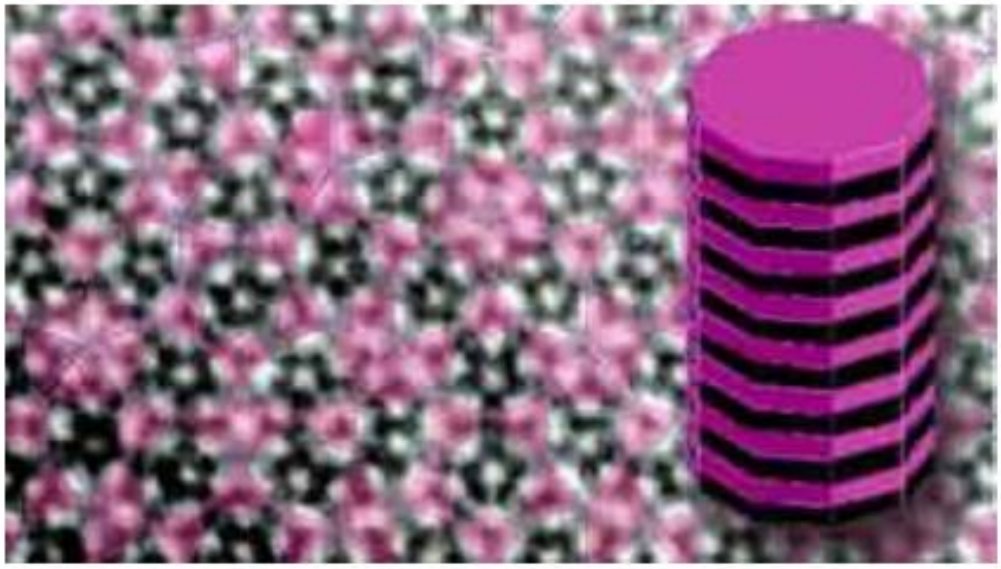

IN THE PLANE, THE AlNiCo QUASICRYSTAL, WHICH CONSISTS OF *OVERLAPPING* DECAGONS, IS APERIODIC. BUT THE STACKED PLANES HAVE PERIODIC STRUCTURE. (EM Images by Steinhardt and Jeong,2000**.** ***Nature*** **,382,**433-35).

quasicrystalline
ordering; by looking at right angles to the planes, they could observe the effects of the periodic, crystalline-like ordering of the stack.

Peter Gille of the Ludwig-Maximilians-University, Munich, grew the quasicrystal, and the samples were prepared and characterized by Horn and by Wolfgang Theis of the Free University of Berlin. At the ALS, Rotenberg, Horn, and Theis examined the samples by means of low-energy electron diffraction and by angle-resolved photoemission at beamline endstation 7.0.1.2.

"Our principal findings were that the distribution of the electronic states in momentum space correlates with the electron diffraction pattern, just like in an ordinary crystal. **The electrons aren't localized to clusters, instead they feel the long-range quasicrystal potential," Rotenberg says.**

"We found that the electrons propagate nearly freely, like conduction electrons in an ordinary metal," he continues, "and we found there is a Fermi surface, crossed by nickel and **cobalt d-electrons**; **its topology should determine some of the material's fundamental properties."**

Band-like properties, common in metals and other ordinary crystals, were not expected in quasicrystals. But then quasicrystals themselves are an unexpected phenomenon.

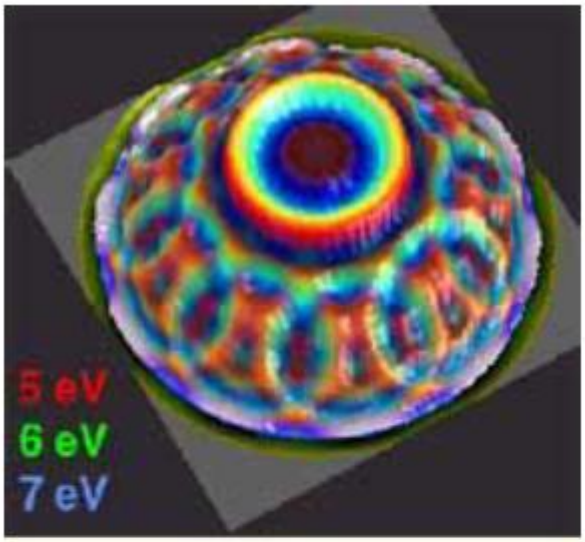

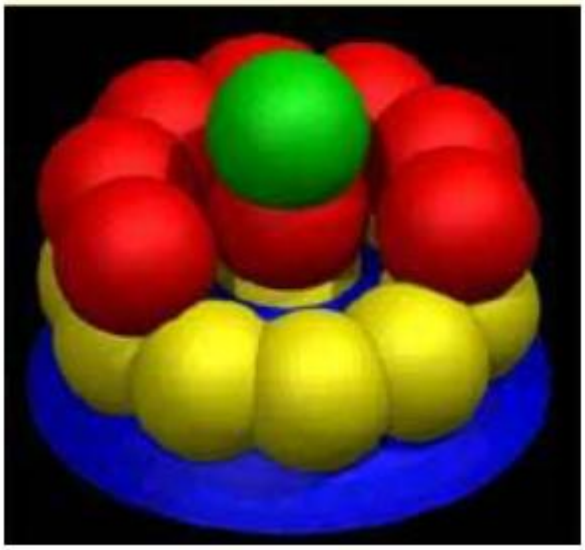

THE CONSTANT ENERGY CONTOURS FOR NEARLY FREE S-P ELECTRONS IN AlNiCo QUASICRYSTALS (DATA, TOP) ARE DERIVED FROM THREE-DIMENSIONAL SPHERES DISTRIBUTED APERIODICALLY IN MOMENTUM SPACE (MODEL, BOTTOM).

"One may predict a quasicrystal structure starting from electrons and quantum mechanics, as approximated by *interatomic pair -potentials* calibrated with *ab initio* total-energy calculations, combined with the experimentally known composition and lattice constants. the 'basic Ni' decagonal phase $d(Al_{70}\ Ni_{21}\ Co_9)$." **[C.L. Henleya, M. Mihalkovic, M. Widom. Total-energy-based structure prediction for d(AlNiCo). *Journal of Alloys and Compounds* 342 (2002)** 221–227 **; www.elsevier.com/ locate/ jallcom].**

3b. Photonic Quasicrystals

BACK TO THE PHOTONIC, ICOSAHEDRAL QUASICRYSTAL MODEL !

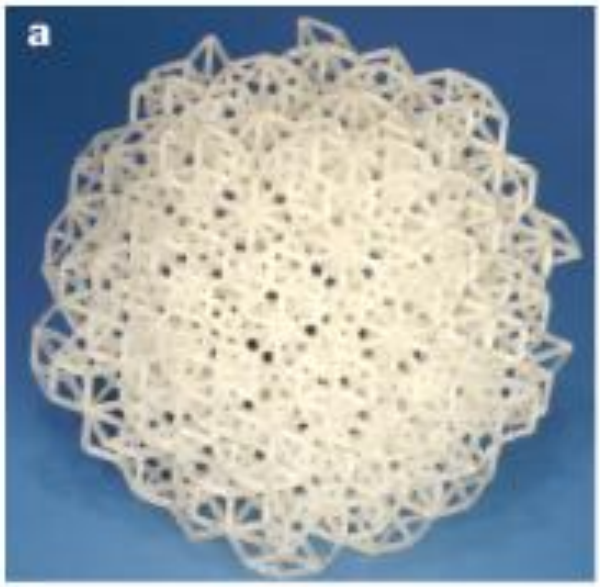

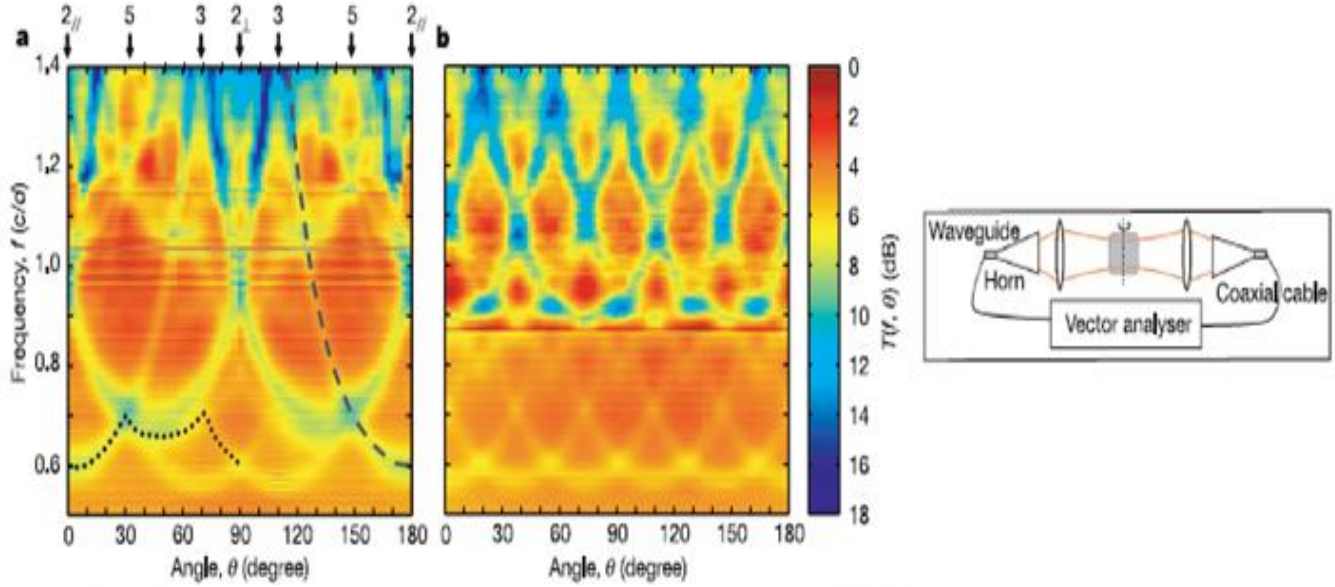

Figure 2 | Measured transmission for an icosahedral quasicrystal. a, $T(f,\theta)$, transmission as a function of frequency (measured in units of c/d) and angle, for a rotation about a two-fold rotation axis of the quasicrystal (corresponding to the dotted line in Fig. 1c) using two overlapping frequency bands. The dashed line is a $1/\cos\theta$ curve characteristic of Bragg scattering from a Brillouin zone face. **b**, $T(f,\theta)$ for a rotation about a five-fold rotation axis corresponding to the dashed line in Fig. 1c. Inset, schematic of the microwave horn and lens arrangement used for these measurements.

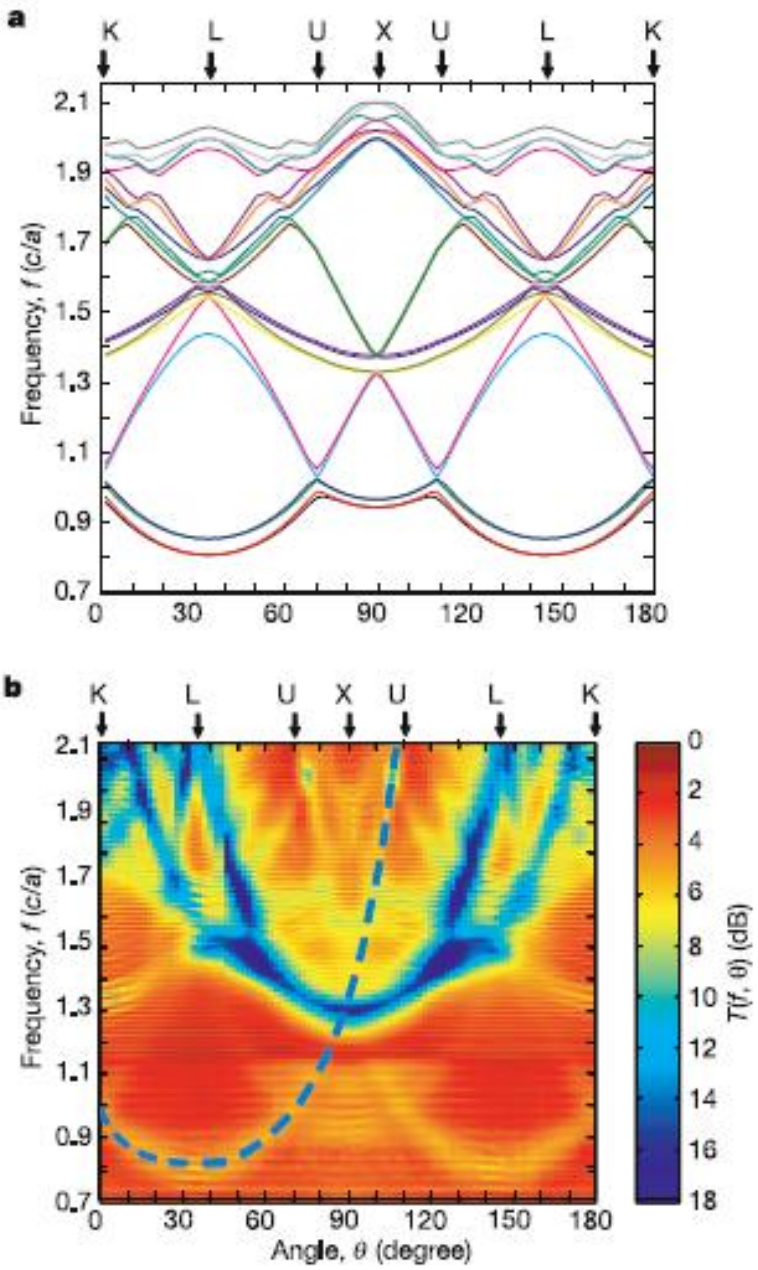

Figure 3 | Comparison of calculated bands and measured transmission for a diamond structure. a, Calculated dispersion relation f on the boundary of the first Brillouin zone versus θ, for the diamond structure along the dotted curve in Fig. 1d. **b**, $T(f,\theta)$ for the sample rotation along the same curve. There is excellent agreement at the photonic gap centre frequencies.

[Source: W. Man et al., *Nature*, 2005 :1 doi:10.1038/nature03977].

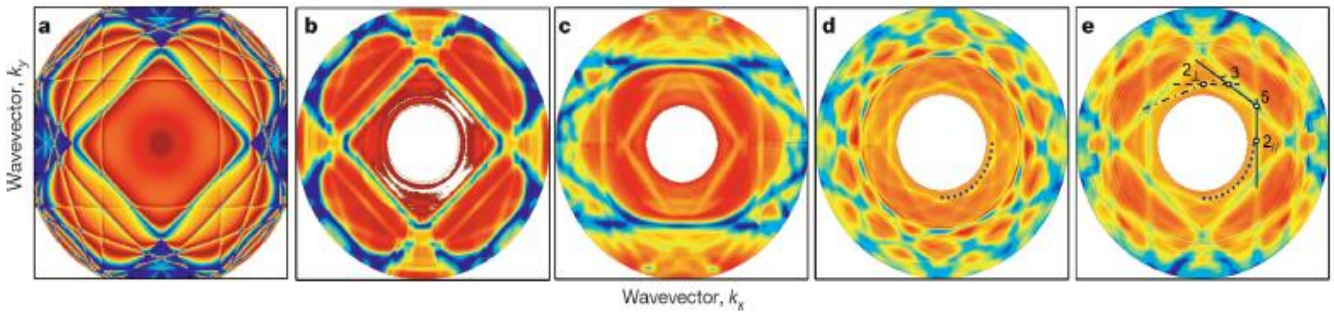

Figure 4 | Imaging of Brillouin zone for diamond and icosahedral quasicrystal structures. a, Brillouin zone for the diamond structure along the four-fold direction as seen in the contour plot of calculated frequency deviation ($\delta f = f - (c/\bar{n})|\mathbf{k}|/(2\pi)$) versus **k**. **b**–**e**, The Brillouin zone can be seen in a plot of the measured $T(r = f, \theta = \theta)$ (using the same scale as Fig. 3) for the diamond lattice along the four-fold (dashed in Fig. 1d) axis (**b**) and two-fold (dotted in Fig. 1d) axis (**c**); and for the quasicrystal along the five-fold (dashed in Fig. 1c) and two-fold (dotted in Fig. 1c) axes (**d**). The inner decagon in **d** and the solid and dashed lines in **e** correspond to the dashed and dotted lines in Fig. 1c. The dash-dotted line is a non-triacontahedral zone face.

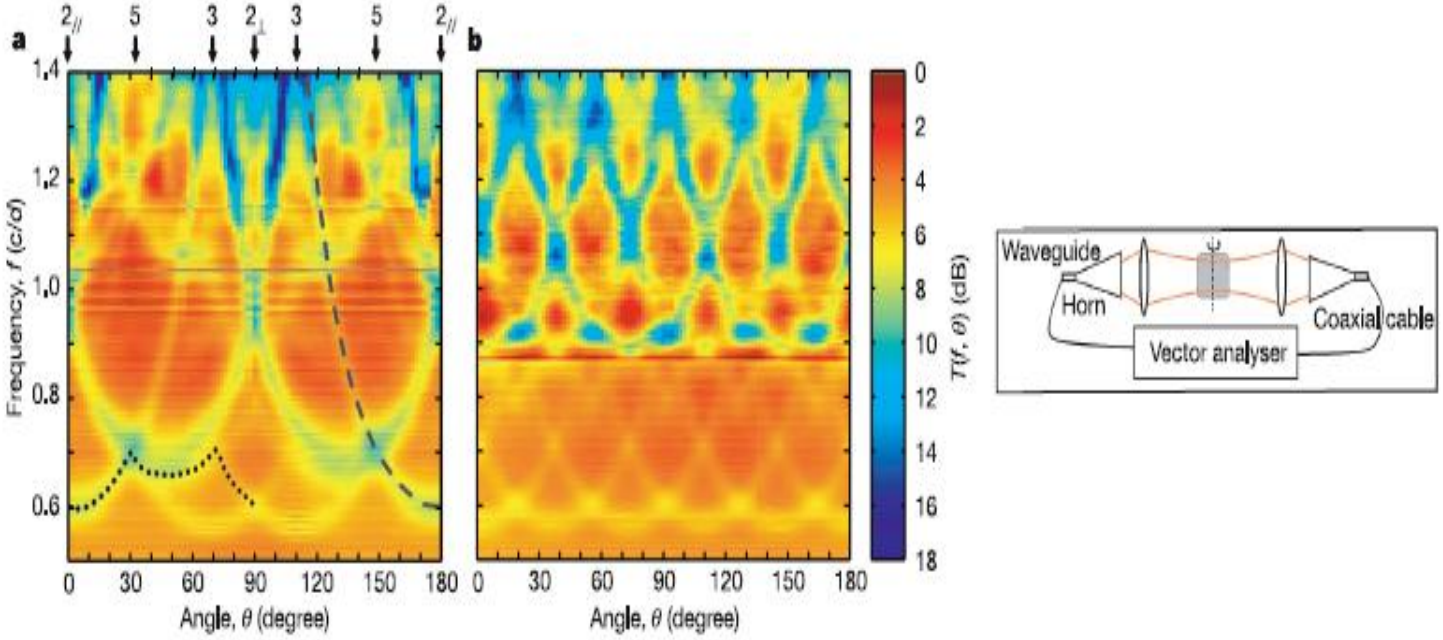

Figure 2 | Measured transmission for an icosahedral quasicrystal. a, $T(f,\theta)$, transmission as a function of frequency (measured in units of c/d) and angle, for a rotation about a two-fold rotation axis of the quasicrystal (corresponding to the dotted line in Fig. 1c) using two overlapping frequency bands. The dashed line is a $1/\cos\theta$ curve characteristic of Bragg scattering from a Brillouin zone face. **b**, $T(f,\theta)$ for a rotation about a five-fold rotation axis corresponding to the dashed line in Fig. 1c. Inset, schematic of the microwave horn and lens arrangement used for these measurements.

4. IONIC and METALLIC GLASSES (my own Data)

4a. LiCl –nH_2O Glasses at 77K, *Chem. Phys. Letts.* (1978)

Instead of only X-ray scattering I have used Solids NMR & Neutron Scattering Data

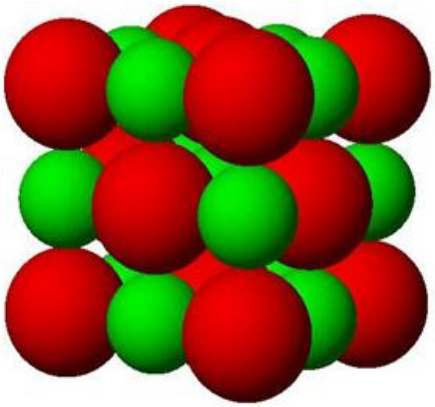

---→ distorted FCC cluster structure

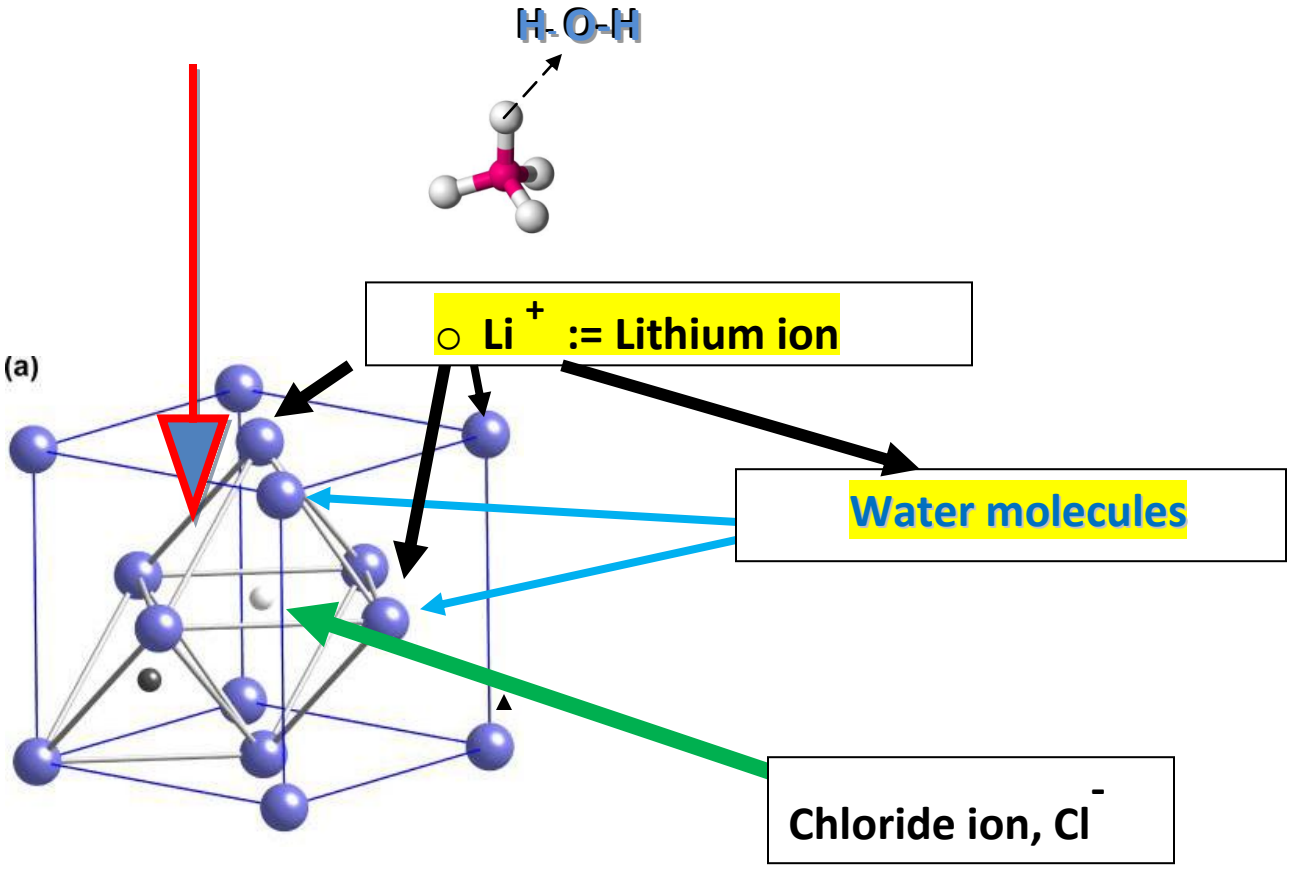

FCC → distortion → LiCl x nH_2O, for 2.2<n< 13 !

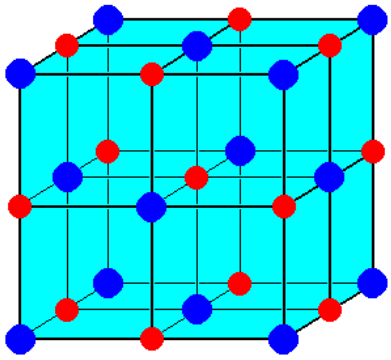

NaCl

r (Cl^-) ~ 1.8 Å , r(Na^+) = 1.0 Å .

4b. Lanthanum Nitrate, $La(NO_3)_3 – nH_2O$ Glasses at 77K, for 4<n<29

The number of electrons in each of Lanthanum's shells is 1s2; 2s2 p6; 3s2 p6 d10; 4s2 p6 d10; 5s2 p6 d1; 6s2 and its electronic configuration is [Xe] $5d^1$ $6s^2$.

La^{+3} has the electronic configuration : 2, 8, 18, 18, 8

Local Structure(s):

Distorted Icosahedra of Hydrated La^{+3} ions with (2 +1) hydration shells:

I(6); II(12) + 3 attached NO_3^- hydrated with 3 water molecules each: Total complex hydration = 27 H_2O !!

I_h:= ….La^{+3} ---18 H_2O + 3 x [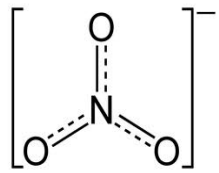 -- 3H_2O].

The hydrated Lanthanum Nitrate x 27H_2O glasses have a local cluster structure which is a distorted version of the ICOSAHEDRAL COORDINATION in the crystal structures of

Ammonium Nitrolanthanates

Ammonium Nitratolanthanates(III)

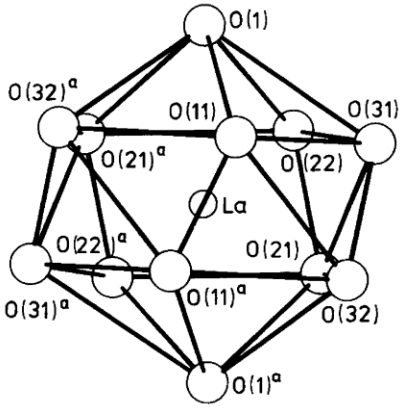

Fig. 4. Coordination polyhedron around the lanthanum atom. (a) A view along the "capping atoms" O(1) and O(1)^a. (b) A view perpendicular to that in (a). The letter *a* refers to the symmetry operation $-x, y, \frac{1}{2}-z$.

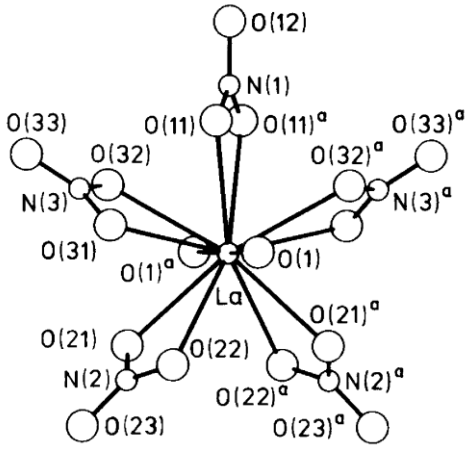

Fig. 1. A perspective view of the $[La(NO_3)_5(H_2O)_2]^{2-}$ complex with the atomic numbering system. The letter *a* refers to the symmetry operation $-x, y, \frac{1}{2}-z$.

Acta Chemica Scandinavica A 36 (1982) 465 — 470

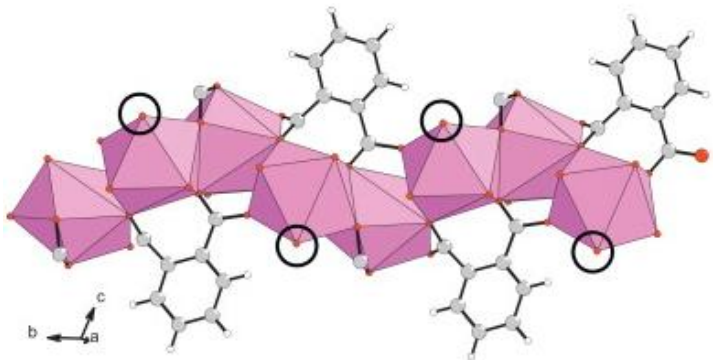

Fig. 6. View of one chain of lanthanide-centered polyhedra running along the *b*-axis in $Nd_2(1,2\text{-bdc})_3(H_2O)_2$ (4). Open circles indicate the additional terminal water bounded to Nd1 and Nd4 cations.

“

The coordination polyhedron around the La atom can be described in both compounds as a slightly distorted icosahedron. This was also the case for the magnesium and potassium compounds. The pattern of the coordinated nitrate groups is, however, different from the potassium compound. In both cases the water molecules occupy *trans* positions of the capping atoms in the icosahedron. In the present complexes each of the five nitrate groups contributes one oxygen atom to each of the two five-membered rings in the icosahedron while in the potassium compound one of the nitrate groups belongs entirely to one of the rings. Fig. 4 shows the coordination polyhedron; distances and angles involved are listed in Tables 3 and 4.

”

- **USES: 1. Lanthanum-rich lanthanide compositions have been used extensively for cracking reactions in FCC catalysts, especially to manufacture low-octane fuel for heavy crude oil. It is utilized in green phosphors based on the aluminate (La0.4Ce0.45Tb0.15)PO_4.**
  - **2. Lanthanide zirconates and lanthanum strontium manganites are used for their catalytic and conductivity properties and *lanthanum stabilized zirconia* has useful electrical and mechanical properties.**
  - **3**. Lanthanum's ability to bind with phosphates in water creates numerous uses in **water treatment**. It is utilized in **laser crystals** based on the **ytrium-lanthanum-fluoride** (YLF) composition. Lanthanum metal is predominantly used in the production of mischmetal and steel additives but is also important in the production of hydrogen storage alloys for **nickel-metal hydride (NiMH) batteries.**

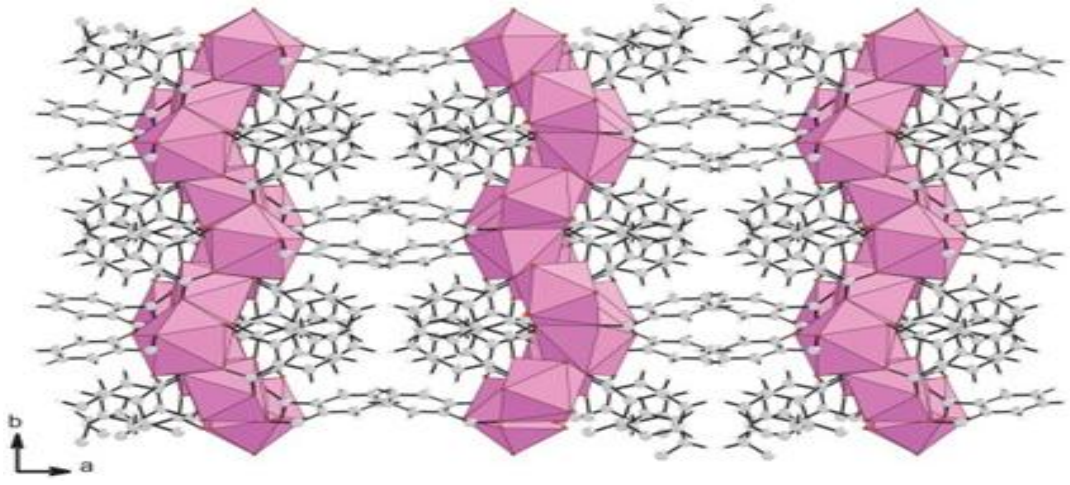

Fig. 4. View of the structure of Ln_2(1,2-bdc)$_3$(H_2O) (1 and 3) along the ***c*** direction, showing the atomic and polyhedral arrangement of the layers of lanthanides with the phthalates groups. *Journal of Solid State Chemistry*, 183 (9) Sept. 2010: 1943–1948

4c. Other Glass Local Structures that I determined in 1977 by Solids NMR at 77K

- $Cd(NO_3)_2 - sH_2O$, s=18,

A distorted Icosahedron, too !

Distorted Octahedra:

- $Zn(NO_3)_2 - mH_2O$ m<13
- $Ca(NO_3)_2 - p\,H_2O$
- $CuCl_2 - qH_2O$ q=6 !

Dynamic Jahn-Teller Effect: the *stable* structure of hexa-hydrated Cu^{+2} is an axially distorted octahedron!

[**Ar**] 3d10 4s1. **A filled or half-filled d shell is more stable**. So, in the most stable configuration the 3p shell takes an electron from the 4s orbital.

4d. Metal Glasses (at the Cavendish Laboratory in 1978-79)

Co_9P-distort.Icosahedra;$FeNiPB, Pd_4Si, Fe_4B, Cu_4Zr$...

- **Co_9P –rod,**

  Quasi-icosahedral (*with shared caps*): from X-ray Scattering (XRS) and Ferromagnetic Resonance

  (**e/a** = (9x2 +4)/10 = **2.20** → icosahedral !, **but P is non-metal** !!)

- **$Fe_{0.6}Ni_{0.2}P_{0.1}B_{0.1}$: XRS and Spin Wave Resonance**

  Fe3 Ni…: e/a ~ (3x 3 +2)/6 = 1.83 … 1.91 → distorted h.c.p. or ~ dodecahedral ?

- **Pd_4Ge from XRS + Neutron Scattering (NS)**

  (e/a = (4 +4)/5= 1.60 → bcc lattice ? , but Germanium is a semiconductor !); perhaps, there is so much metal in the glass that the metallic character apparently predominates, but there are neither Brioullin zones nor Bloch waves in metallic glasses?!

- **Pd_4Si from XRS and NS**

- **Fe_4B**

- **Cu_4Zr**

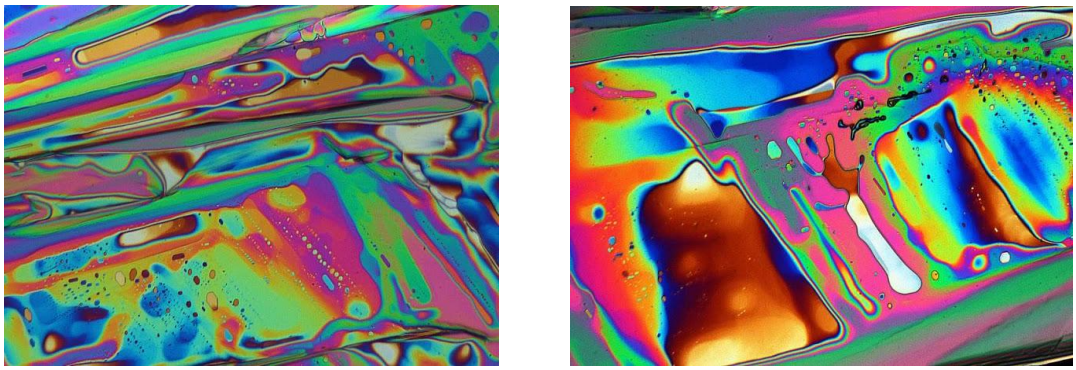

Lanthanum Nitrate Hexahydrate –80 x Polarized Light Micrograph:

``***Lanthanum* (III) *nitrate* hexahydrate ($La(NO_3)_3$)** *is a strange compound!"*

Only 24 Bravais crystal lattices ➔ 230 crystallographic (or *space*) groups

(only 14 crystal lattices are shown here !)

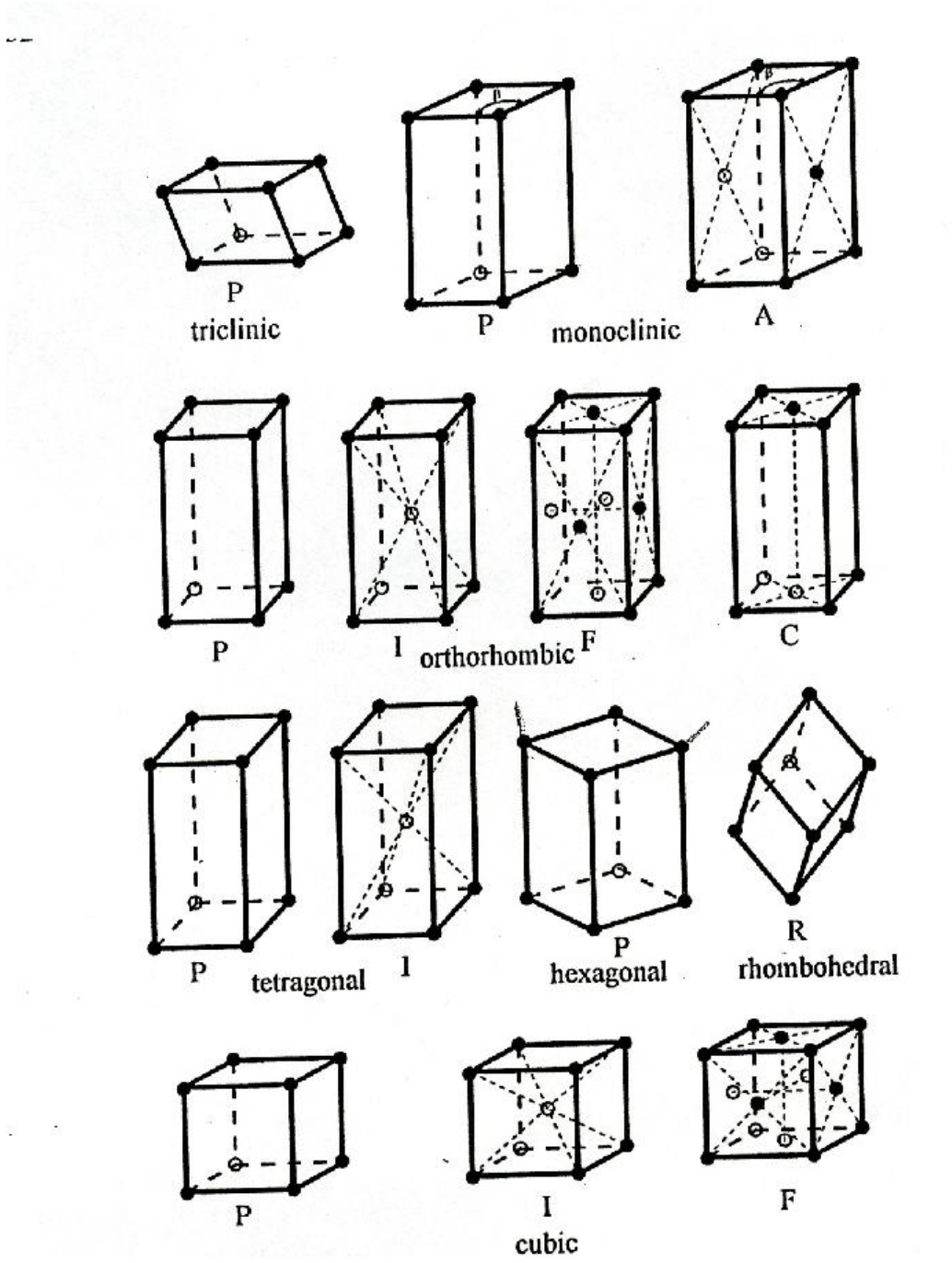

There are many more *quasicrystalline* arrangements of atoms possible, corresponding to some 776+… *superspace* groups up to 6D.

5. CONCLUSIONS

1. **Icosahedral structures, *albeit* distorted, were observed in both hydrated *Lanthanide crystals and ionic glasses* a full 7 to 20 years prior to the reporting of the icosahedral quasicrystalline structure of $Al_{0.14}Mn_{0.86}$ ($Al_{14}Mn_{86}$ ~Al_6Mn) in 1984.**
2. **Both quasicrystals and metallic glasses (e.g., $Ni_{67}Zr_{33}$) have Pseudo Brillouin zone(s) and a Fermi pseudo-gap.**

3. **The *stability* of the quasicrystalline and of crystalline metal alloys depends in a systematic manner on the electron distribution in these systems, and can be predicted surprisingly well from e/a values—the average number of valence electrons per atom-- for a wide range of binary alloys, from CuAl alloys, to brasses, and to AlTM alloys (including quasicrystalline Al_6Mn) for the entire series of transition metals (TMs) that are `*Hume-Rothery complex alloys'*. It seems that *ab initio* quantum computations are now possible for all such metal alloy structures, fulfilling Hume-Rothery's dream from 1936!**

4. **In ionic glasses with water, quasicrystals and crystals the close packing of atoms and the valence electron interactions result in stable or meta-stable coordination structures that cover the complete range of Platonic polyhedra, *albeit* often in *distorted* forms, thus deviating from the ideal polyhedra.**

5. **Aside from *ab initio* computations, there is plenty of scope for *geometric* and *topological* approaches to these systems.**
   (Mathematics is thus *neither* Platonic nor it is an ivory tower!)

Evans et al. (1979) Pseudopotential-based computations for CuAl alloys:

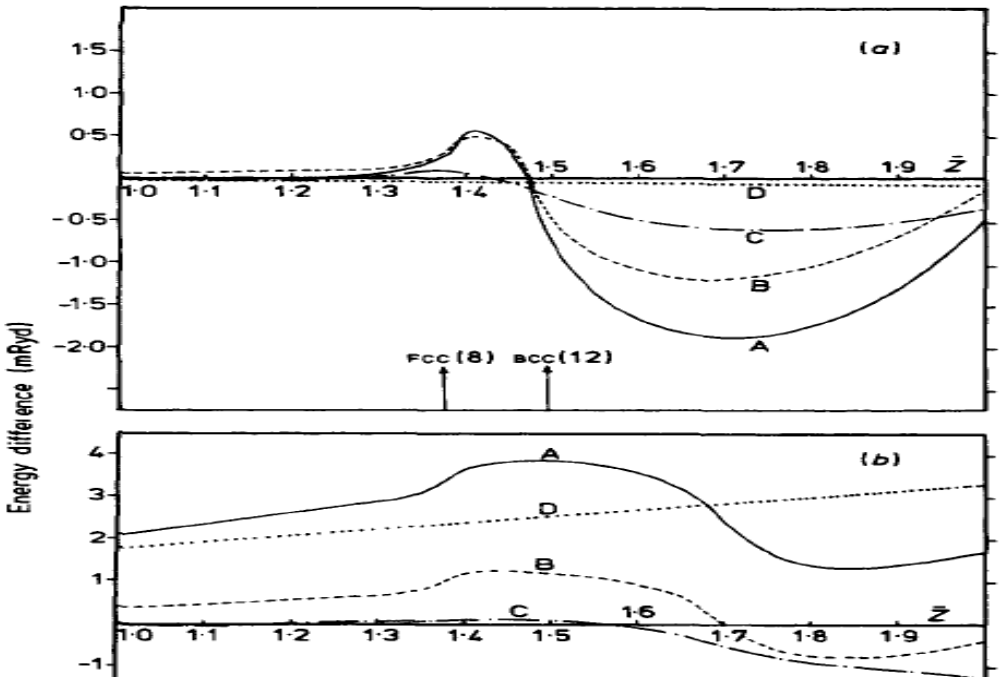

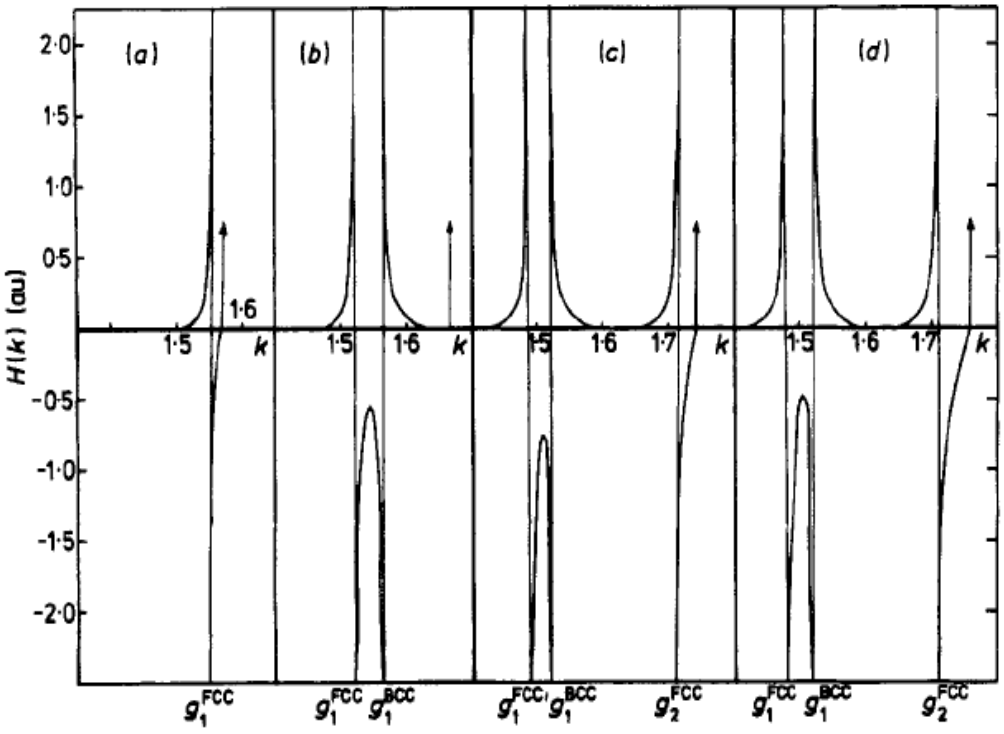

Figure 5. The integrand $H(k)$ (equation (41)) plotted for a range of wave vectors k and several values of the electron/atom ratio $\bar{Z}$ for CuAl: (*a*), $\bar{Z} = 1{\cdot}4$ (FCC favourable); (*b*), $\bar{Z} = 1{\cdot}8$ (BCC favourable); (*c*), $\bar{Z} = 2{\cdot}2$ (BCC favourable); (*d*), $\bar{Z} = 2{\cdot}3$ (BCC ~ FCC). The calculations are based on the Thomas–Fermi approximation to the screened pseudopotentials. The arrows in each diagram denote the position of $2K_F$, and the positions of the relevant reciprocal lattice vectors $\boldsymbol{g}$ are indicated. Note that the $\boldsymbol{g}$'s vary with concentration since the atomic volume of the alloy changes.

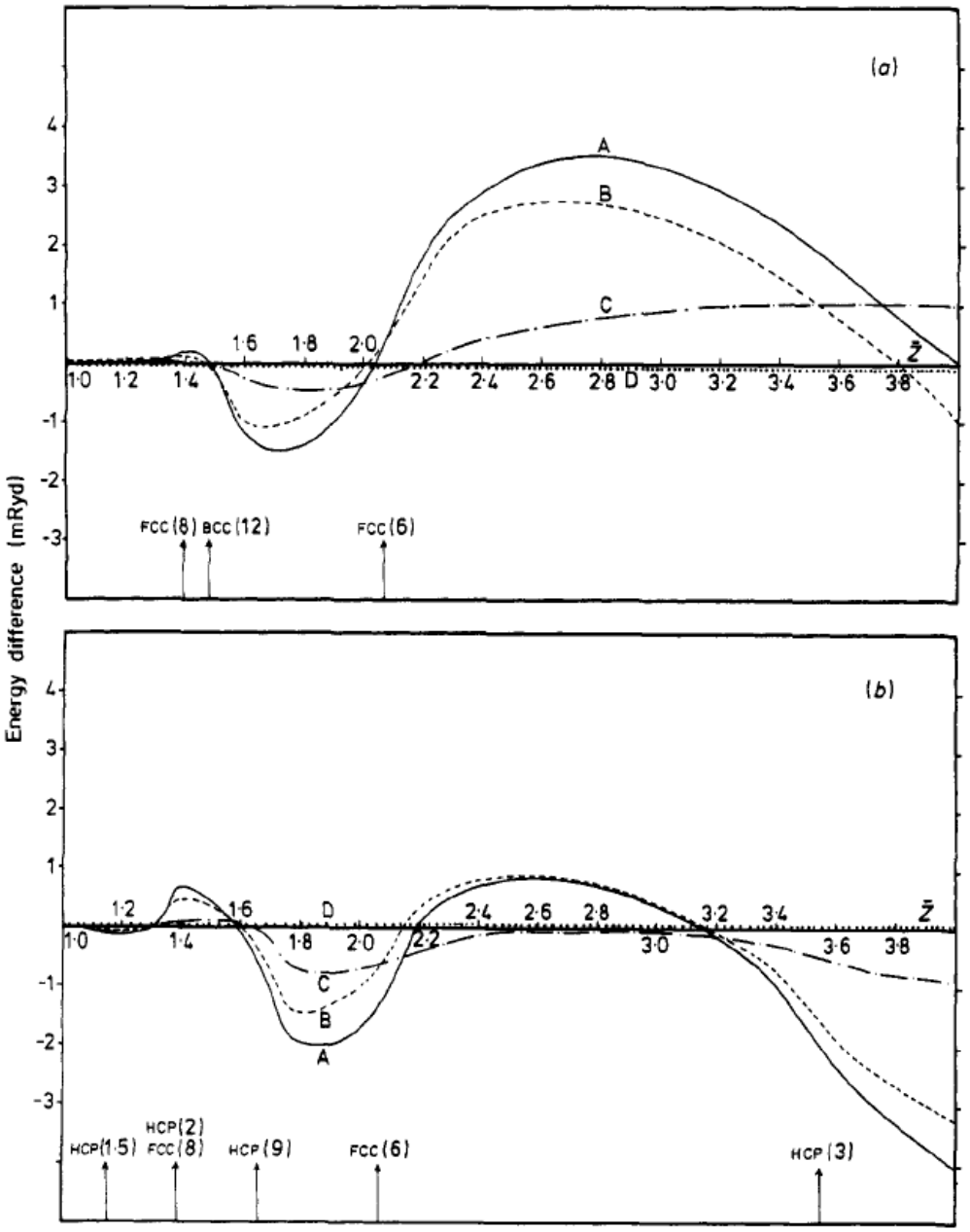

Figure 3. (*a*), the free energy difference per electron $F^{BCC} - F^{FCC}$ for CuSn as a function of the electron atom ratio $\bar{Z}$. The calculations use the Ashcroft empty-core pseudopotential with $r_c^{Cu} = 1{\cdot}24$ au and $r_c^{Sn} = 1{\cdot}30$ au. The labelling of the curves follows that in figure 1(*a*). (*b*), the free energy difference per electron $F^{HCP} - F^{FCC}$ for CuSn as a function of the electron per atom ratio $\bar{Z}$. The *c*/*a* ratio is taken to be the ideal ratio for all concentrations. The labelling of the curves follows that in figure 1(*a*).

CuSn Alloys

CuZn Alloys

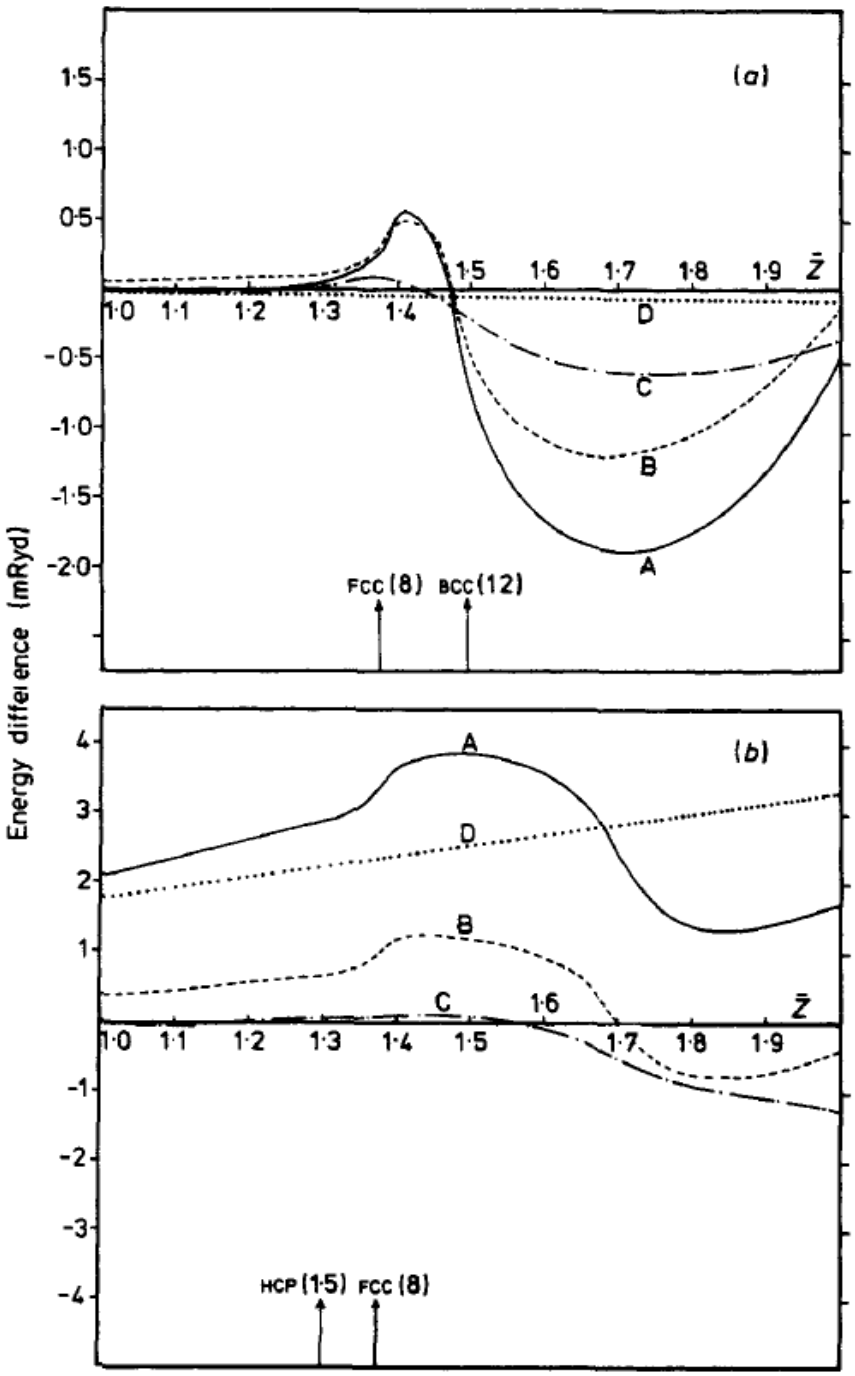

Figure 2. (*a*), the free energy difference per electron $F^{BCC} - F^{FCC}$ for CuZn as a function of the electron/atom ratio $\bar{Z}$. The calculations use the Ashcroft empty-core pseudopotential with $r_c^{Cu} = 1{\cdot}24$ au and $r_c^{Zn} = 1{\cdot}27$ au. The labelling of the curves follows that in figure 1(*a*). (*b*), the free energy difference per electron $F^{HCP} - F^{FCC}$ for CuZn as a function of the electron/atom ratio $\bar{Z}$. The *c*/*a* ratio is taken to be 1·857, the value observed for pure Zn, at all concentrations. The labelling of the curves follows that in figure 1(*a*).

Hamlet: ***"And therefore as a stranger give it welcome.*** *There are more things in heaven and earth, Horatio, than are dreamt of in your philosophy*." (William Shakespeare)

References

- Kittel, Charles (1996). *Introduction to Solid State Physics*. New York City: Wiley. ISBN 0-471-14286-7.
- Ashcroft, Neil W.; Mermin, N. David (1976). *Solid State Physics*. Orlando: Harcourt. ISBN 0-03-049346-3.
- Brillouin, Léon (1930). "Les électrons dans les métaux et le classement des ondes de de Broglie correspondantes" (http://gallica.bnf.fr/ark:/12148/bpt6k31445). *Comptes Rendus Hebdomadaires des Séances de l'Académie des Sciences* **191** (292).
- Setyawan, Wahyu; Curtarolo, Stefano (2010). "High-throughput electronic band structure calculations: Challenges and tools". *Comp. Mat. Sci.* **49**: 299–312. doi:10.1016/j.commatsci.2010.05.010.

Elke Koch & Werner Fischer. ***Mathematical Crystallography***.
http://www.staff.uni-marburg.de/~fischerw/minsurfs.htm
http://www.staff.uni-marburg.de/~fischerw/mathcryst.htm

ADDITIONAL LITERATURE

[1] Scopigno,T. J.-B. Suck, R. Angelini, F. Albergamo, G. Ruocco. 2006-2008. High Frequency **(THz)** dynamics in metallic glasses (**$Ni_{0.33}$ $Zr_{0.67}$**). 10.1103/PhysRevLett.96.135501. http://arxiv.org/abs/cond-mat/0603251 (The crystalline phase is **$NiZr_2$**, **but it is *glassy* for $Ni_{0.24}$ $Zr_{0.76}$**). *"In these pioneering experiments it was possible to prove the existence of* **Pseudo Brillouin Zones** with **clear Zone Boundaries** *near the maxima of the static structure factor, these latter acting like "***smeared out lattice points**" [3]. J. Hafner, ***J. Physics C* 16**, 5773 (1983).

[2] T. Otomo, M. Arai a J.-B. Suck , S.M. Bennington. 2002. An experimental approach to reveal the origin of collective excitations in Ni_{33} Zr_{67} metallic glass. *Journal of Non-Crystalline Solids* **312–314**: 599–602. (**INS**).

[3] Boca, F.P., Zaharescu, A. 2007. The distribution of the free path lengths in the periodic two-dimensional Lorentz gas in the small-scatterer limit, Commun. Math. Phys., 269: 425-471.

[4] Boca, F.P. 2008. **An AF algebra associated with the Farey tessellation**, *Canadian J. Math*., **60**: 975-1000.

[5] Boca, F.P. 2010. **The distribution of the linear flow length in a honeycomb in the small-scatterer limit**, *New York J. Math.,* **16**: 651-735.

[6] Baianu, I.C. 1978. **X-ray scattering by partially disordered membrane systems**, *Acta Cristallographica*, **A34** (5): 751-753.

[7] Baianu, I.C., Glazebrook, J.F., Brown, R. 2009. Algebraic Topology Foundations of Supersymmetry and Symmetry Breaking in Quantum Field Theory and Quantum Gravity, Symmetry, *Integrability and Geometry: Methods and Applications* (*SIGMA*), **5**: 1-70 (051); doi:10.3842/SIGMA.2009.051.
[8] Baianu, I.C. 2011. A Quantum Algebraic Topology Framework for Multiscale Quantum Computations, *International Journal of Mathematics and Computational Methods in Science & Technology*, **3**: 1-24.
[9] Baianu, I.C., Glazebrook, J.F., Brown, R. 2011. Quantum Symmetries, Operator Algebra and Quantum Groupoid Representations: Paracrystalline Systems, Topological Order, Supersymmetry and Global Symmetry Breaking, *Intl. J. Rev. Res. Appl. Sci. (IJRRAS),* **9** (2): 1-44. http://www.arpapress.com/Volumes/Vol9Issue2/IJRRAS 9 2 01.pdf.
[10] Baianu, I.C. 2012. **Paracrystalline Nanostructure and Dynamics,** *Nanoscience and Nanotechnology*, **2**: 11-41.
Taylor & Francis Publishers: Boca Raton, FL.
[11] Ashmead, J. 2012. Morlet Wavelets in Quantum Mechanics, *Quanta*, **1**: 58-70.
[12] Shechtman, D., Blech, I., Gratias, D., Cahn, J. W. 1984. **Metallic phase with long-range orientational order and no translational symmetry**, *Phys. Rev. Lett*., **53**: 1951-1954.
[13] Senechal, M. 1995. ***Quasicrystals and Geometry***, Cambridge University Press: Cambridge, UK.
[14] Stadnik , Z.M. 1999. ***Physical Properties of Quasicrystals***, Springer: Berlin.
[15] Steurer, W., Deloudi, S. 2008, ***Fascinating quasicrystals***, *Acta Cristallographica*, **A64**: 1-11.
[16] Steurer, W., Deloudi, S. 2009. ***Crystallography of Quasicrystals***, Springer: Berlin.
[17] Mizutani, U. 2010. ***Hume-Rothery Rules for Structurally Complex Alloy Phases***, Springer: Berlin.
[18] Sunada, T. 2012. **Crystals That Nature Might Miss Creating**. *Notices of the Amer. Math. Soc*., **55** (2): 208-215;
Lecture on Topological Crystallography, *Japanese Journal of Mathematics*, 7: 1-39.
[19] Moody, R. V., Nesterenko, M., Patera, J. 2008. **Computing with almost periodic functions**, *Acta Crystallographica*, **A64**: 654-669.
[20] de Bruijn, N. G. 1986. **Quasicrystals and their Fourier transform**, *Nederl. Akad. Wetensch. Indagationes Math*.,
48 (2): 123-152.
[21] Golse, F. 2012. Recent results on the periodic Lorentz gas, in *Nonlinear Partial Differential Equations (Advanced Courses in Mathematics - CRM* Barcelona), pp. 39-99, Springer, Basel.
[22] Marklof, J., Str¨ombergsson, A. 2010. The distribution of free path lengths in the periodic Lorentz gas and related lattice point problems, *Annals of Mathematics*, **172**: 1949-2033; 2011. The Boltzmann-Grad limit of the periodic Lorentz gas, *Annals of Mathematics*, **174**: 225-298.
[23] Wennberg, B. 2012. **Free path lengths in quasicrystals**, *J. Statistical Physics*, **147**: 981-990.